Archaeologia Polona, vol. 54: 2016, 137–150
PL ISSN 0066-5924

Archaeometric study of some functional tools from the Sąspów and Wierzbica 'Zele' flint mines sites

Jolanta Małecka-Kukawka[a], Grażyna Szczepańska[b], Marta Rauchfleisz[b] and Łukasz Kowalski[a]

In the present work, an archaeometric approach was used to investigate a sample of the functional tools collected from the Sąspów, Cracow district, and Wierzbica 'Zele', Radom district, flint mines sites. The investigated collection was completed on four non-use-worn specimens. The presence of areas enriched in iron (Fe) compounds has been noticed on the surfaces of all the specimens. They were analyzed by optical microscopy (OM) and scanning electron microscopy (SEM) coupled with an energy dispersive X-ray analysis system (EDS). Data sets were statistically evaluated using similarity analysis (DA, CA, MDS). The results indicated the variables that best discriminate the investigated flint artifacts collection in terms of either anthropoghenic or non-anthropoghenic nature of the residues preserved on their surfaces.

KEY-WORDS: use-wear analysis, residue analysis, SEM-EDS, archaeometry, flint mining

MATERIALS

The collection investigated here consist of two functional tools from the Sąspów, Cracow district (Dzieduszycka-Machnikowa and Lech 1976) and Wierzbica 'Zele', Radom district (Lech 1995: 465–480) flint mine sites and, for controlled comparison, four other non-use-worn specimens (Tab. 1 and Fig. 1). The presence of maroon-colored stains is clearly noticeable on the working edges and surfaces of all the specimens (Fig. 2). In our preliminary opinion, there is likely to be a correlation between the stains and the iron (Fe) enriched compounds. Since such areas are present on the working edges of functional tools (K_1 and K_2) only, it provides us a basis to consider them in terms of residues; defined here as non-parent materials adhered to or incorporated on the surface of a tool (Evans and Donahue 2005: 1734).

[a] Nicolaus Copernicus University, Institute of Archaeology, Szosa Bydgoska 44/48, 87-100 Toruń, Poland
[b] Nicolaus Copernicus University, Faculty of Chemistry, PAI Instrumental Analyses Laboratory, Gagarin 7, 87-100 Toruń, Poland

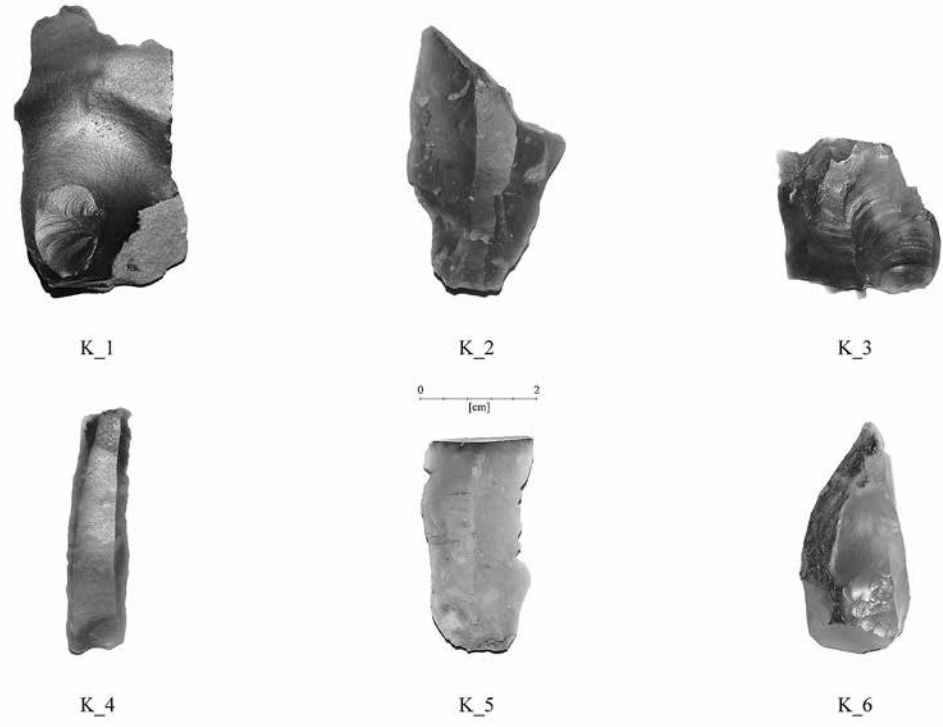

Fig. 1. The studied flint tools (K_3 and K_6 scaled as 3/2 with P_4 as 2/1). Photo: Ł. Kowalski.

Table 1. A comparision of the studied artifacts (N – Neolithic; EBA – Early Bronze Age; LBA – Late Bronze Age; EIA – Early Iron Age).

Artifact	Site	Province	Chronology	Raw material	Typology	Use-wear	Function
K_1	Wierzbica 'Zele'	Mazovia	LBA - EIA	'chocolate' flint	Flake	Yes	Scraper
K_2	Sąspów 1	Lesser Poland	N	Jurrasic-Cracow flint	Blade (bulb part)	Yes	Scraper
K_3	Toruń-Gręboc in 243	Kuyavia-Pomerania	EBA	Baltic erractic flint	Flake	No	-
K_4	Skrzypkowo 13	Kuyavia-Pomerania	N - EBA	Baltic erractic flint	Blade	No	-
K_5	Skrzypkowo 13	Kuyavia-Pomerania	N - EBA	Baltic erractic flint	Blade	No	-
K_6	Toruń-Gręboc in 243	Kuyavia-Pomerania	EBA	Baltic erractic flint	Flake	No	-

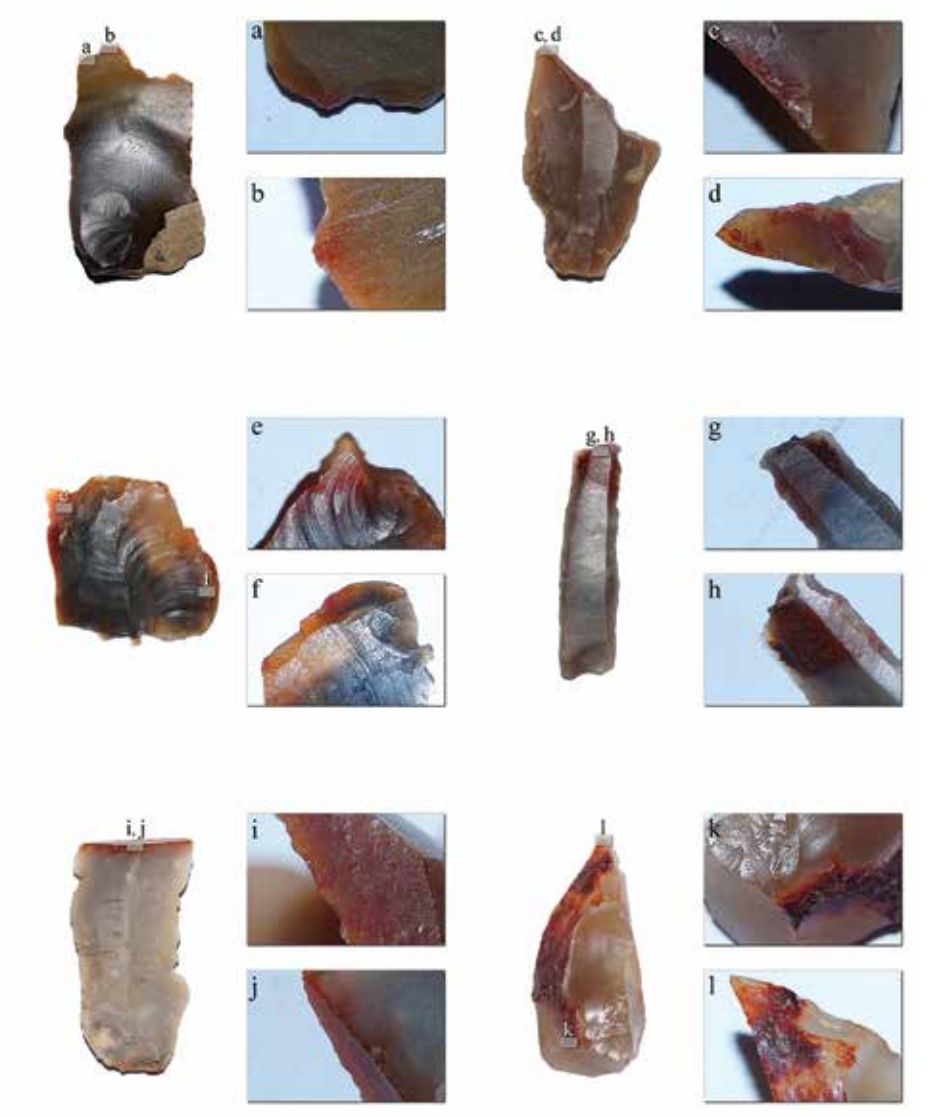

Fig. 2. The studied flint tools. Zoom in on the areas enriched in the iron (Fe) compounds. Photo: Ł. Kowalski.

METHODS

Use-wear analysis

Use-wear analysis (traceology) is an analytical method that allows the identification and interpretation of anthropogenic traces remaining on the surface of non-metallic tools (e.g., those made of silica, stone and organic raw materials). Use-wear analysis is also concerned

with a wide range of deformations which might occur during the tools transport, deposition etc. (Małecka-Kukawka 2012: 464–471). Premilinary use-wear research was performed using a Nikon SMZ 2T stereomicroscope. Optical observations on the functional tools were carried out using a Zess Axiotech in reflection mode equipped with a AxioCam ICc 3 digital camera supported by an AxioVision 4.0 software. For identifying the use-wear profile of functional tools, the observations were directed on the working edges and areas just adjacent to the use-worn zone with optical imaging performed in the reflected light mode.

Laser ablation

Laser ablation technique was performed prior to the SEM-EDS investigations. As a result of impacting a high energy laser beam on a tool surface the removal (without a liquid state) of a secondary type residue (accumulated during pre- or postdepositional process) was completed.

Laser ablation was performed with a system for solid-state layers LSX-213 (CETAC Technologies, USA) equipped with Neodymium-pulsed Laser Nd:YAG. For ablating two scanning lines the laser was used at 755 V energy level and ablated at a speed of 100 μm/s, with a spot size set at 150 μm in diameter.

The ablation was carried out at two locations on each tool surface. The first was an area on the dorsal surface selected away from any locus exhibiting use-wear. The second

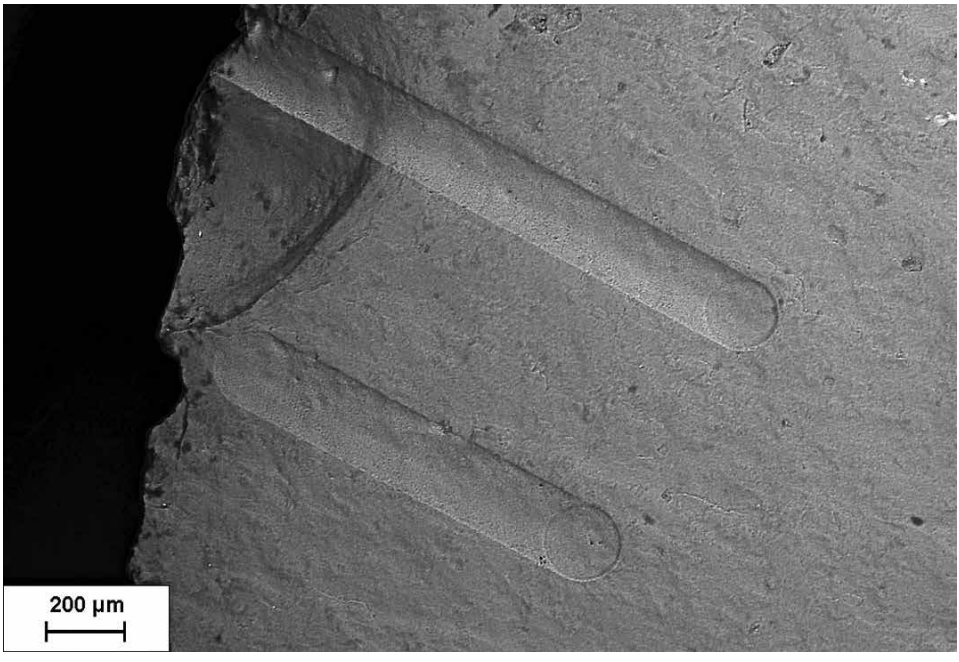

Fig. 3. The surface of sample K_1 with a visible ablated area. Photo: G. Szczepańska.

location was along an edge where use-wear analysis had confirmed surface polishing. The two areas were selected on the same tool since they are likely to have undergone the same post-depositional process (refer with Evans and Donahue 2005). For the non-archaeological specimens, the ablation was carried out on the surface selected away from any exibiting iron (Fe) enriched compounds. K_4 specimen was also ablated within the area enriched in Fe compounds. An exemplary ablated area is given in Fig. 3.

SEM-EDS

The SEM imaging was performed using a scaninnig electron microscope LEO 1430VP (Zeiss). Surface observations were carried out by means of a BSE detector with 28kV accelerating voltage and environmental vacuum mode (the chamber pressure of 50Pa). X-ray microanalyses were conducted using an EDS spectrometer Quantax 200 with XFlash 4010 detector (Bruker AXS) coupled with the scaninnig electron microscope LEO 1430VP (Zeiss). The EDS investigations were performed in semi-quantitative, surface and standardless mode completed by non-conducting material imaging using a BSE detector with pressure of 50Pa. The SEM-EDS was applied in order to achieve a chemical profile of the matrices and enriched areas (EA) including elemental mapping images.

RESULTS

The use-wear analysis results are in accordance with preliminary macroscopic observations indicating an absence of use-wear traces on the K_3-K_6 specimens. For the working edges of the functional tools (K_1 and K_2) the presence of a polish has been recognized. Due to a use-wear profile of the traces left on the functional tools, it is highly likely that both the K_1 and the K_2 were used to scrape an abrasive material (Małecka-Kukawka 2011: 139–147).

A polish present on the K_2 surface is indicative of a long-term use having been arranged along a working edge with smooth and greasy texture and with noticeable parallel strations (Fig. 4e–h). Unlike the well-formed K_2 polish, the one present on the working edges of K_1 exhibits a rough and greasy texture and no visible strations (Fig. 4a–d; see also van Gijn 1989) and therefore may reflect a short-term use of the tool.

Analytical areas for laser ablation and SEM-EDS investigations were selected based on the use-wear analysis results. Elemental mapping images for aluminum (Al), silicon (Si) and Fe distribution were obtained during the SEM research (Fig. 5).

The EDS investigations were performed in three analytical areas: (1) non-ablated silica matrix, (2) ablated silica matrix and (3) non-ablated enriched area and also for K_4 only in ablated enriched area. The resulting elemental weight fractions, excluding carbon (C), were converted to the corresponding oxide weight fractions and normalized to 100 (refer with Tab. 2).

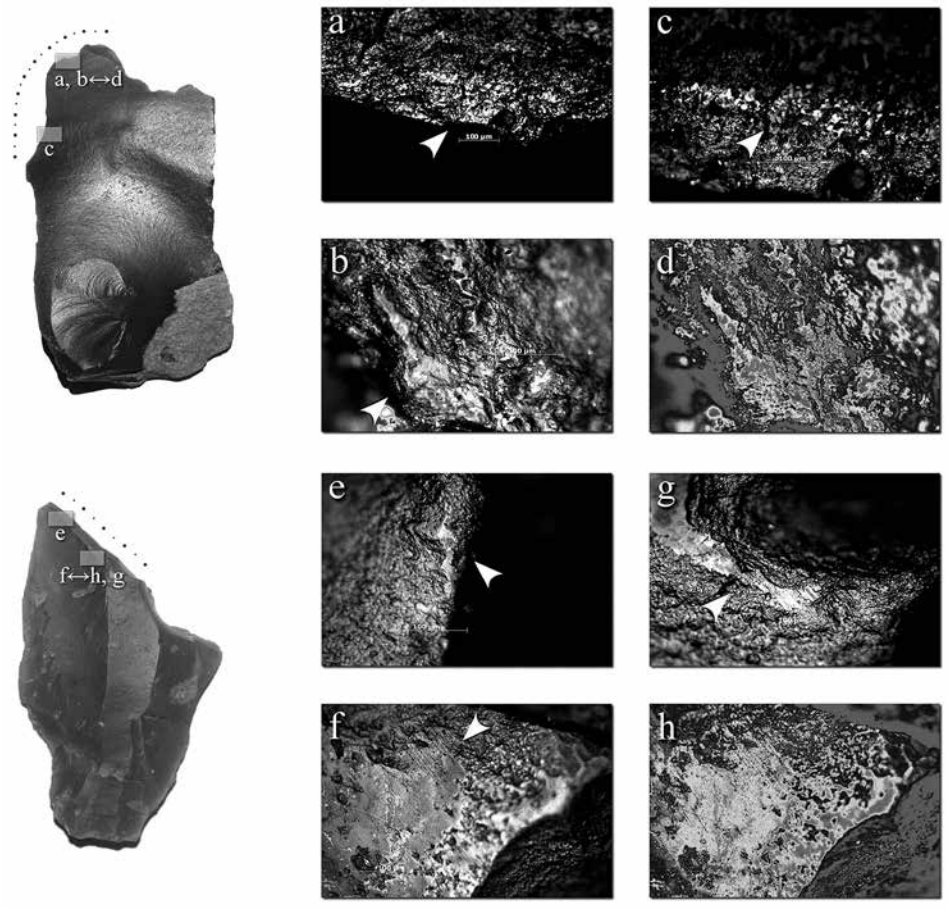

Fig. 4. The optical images of samples K_1 (a–d) and K_2 (e–h) working edges with a visible initial polish (a–d) and well-formed polish (e, g) with the noticeable parallel strations (f, h). Photo: J. Małecka-Kukawka and Ł. Kowalski.

Fig. 5. The SEM images of the EA for the selected tools with the corresponding elemental mapping images. Photo: G. Szczepańska and Ł. Kowalski.

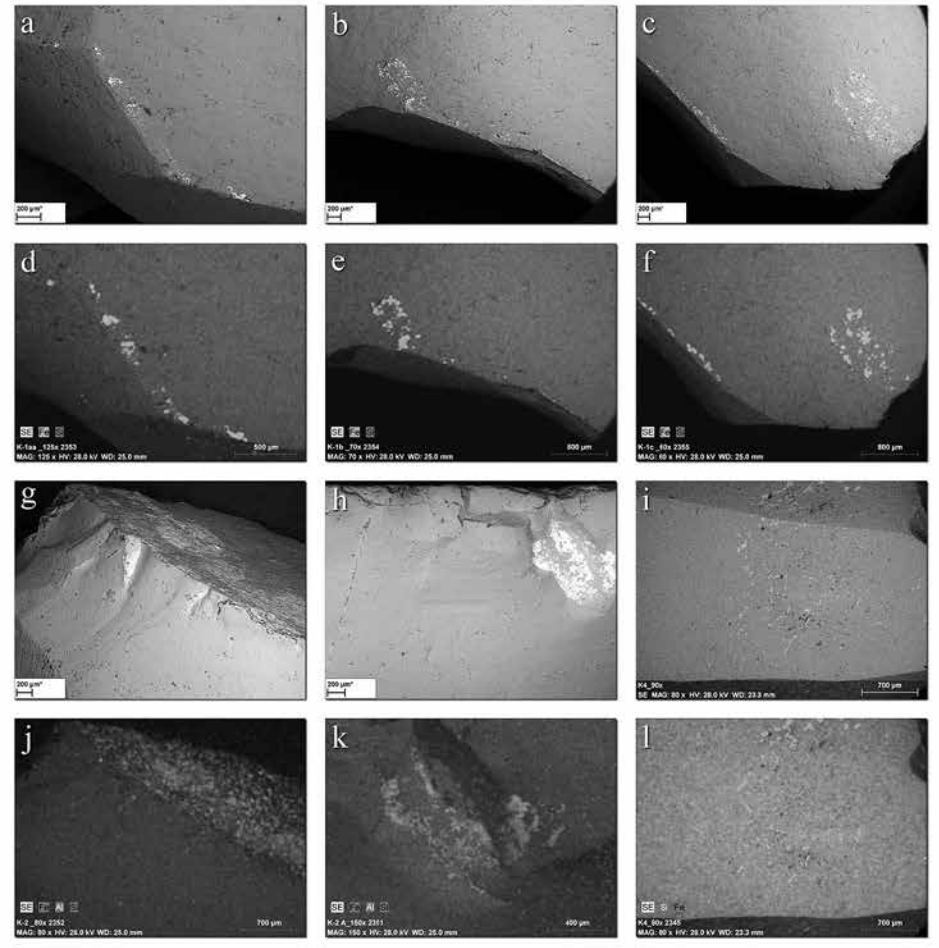
a
b
c
d
e
f
g
h
i
j
k
l


a, d
b, e
c, f
g, j
h, k
i, l
K_1
K_2
K_4

Table 2. The oxide weight fractions (wt%) according to the EDS (M – silica matrix; EA – area enriched with a high Fe content; < DL – concentration below a detection limit; n-a – non-ablated area; a – ablated area).

Artifact	Area		C	MgO	Al_2O_3	SiO_2	P_2O_5	K_2O	CaO	MnO	Fe_2O_3
	Type	Preparation									
K_1	M	n-a	0,21	< DL	3,1	95	< DL	0,47	0,38	< DL	0,85
K_1	M	n-a	2,8	< DL	3,8	92	< DL	0,30	< DL	< DL	0,64
K_1	M	a	0,11	< DL	3,8	95	< DL	0,27	0,15	< DL	0,47
K_1	M	a	0,10	< DL	4,6	94	< DL	0,25	0,20	< DL	0,40
K_1	EA	n-a	3,3	0,74	5,0	48	< DL	0,22	0,36	0,59	42
K_1	EA	n-a	5,8	0,67	13	47	< DL	0,45	0,73	0,43	32
K_2	M	n-a	6,8	< DL	1,5	92	< DL	< DL	< DL	< DL	< DL
K_2	M	n-a	3,7	< DL	1,6	95	< DL	< DL	< DL	< DL	< DL
K_2	M	a	3,5	< DL	1,7	95	< DL	< DL	< DL	< DL	< DL
K_2	M	a	4,1	< DL	1,5	94	< DL	< DL	< DL	< DL	< DL
K_2	EA	n-a	7,3	< DL	1,3	74	< DL	0,19	0,35	< DL	17
K_2	EA	n-a	9,8	1,3	5,5	37	< DL	0,23	0,52	0,62	45
K_3	M	n-a	4,6	< DL	3,8	90	0,10	0,30	0,28	< DL	0,86
K_3	M	a	18	1,1	7,6	67	0,73	2,5	1,8	< DL	1,6
K_3	EA	n-a	6,4	1,5	9,2	64	0,78	0,52	0,33	< DL	17
K_4	M	n-a	5,3	< DL	1,4	93	< DL	< DL	< DL	< DL	0,45
K_4	M	a	13	< DL	2,1	81	< DL	0,48	0,41	< DL	2,6
K_4	M	a	11	< DL	2,2	85	< DL	0,44	0,48	< DL	1,5
K_4	EA	n-a	5,1	< DL	2,8	67	0,76	0,41	0,28	< DL	23
K_4	EA	a	3,4	< DL	3,8	68	0,99	0,47	0,28	< DL	23

K_5	M	n-a	5,2	< DL	1,8	92	< DL	< DL	< DL	< DL	0,72
K_5	M	a	4,2	< DL	1,3	94	< DL	< DL	< DL	< DL	0,70
K_5	M	a	3,7	< DL	1,4	94	< DL	< DL	< DL	< DL	0,61
K_6	M	n-a	2,9	0,79	11	84	< DL	0,36	< DL	< DL	1,5
K_6	M	a	2,1	0,20	8,6	87	< DL	0,34	< DL	< DL	2,0

Table 3. The factor structure matrix for the analytical areas ($Var._{cum.}$ – cumulative variance; n/a – not applicable due to a high value of partial correlation).

Area	Root	$Var._{cum}$	MgO	Al_2O_3	SiO_2	P_2O_5	K_2O	CaO	MnO	Fe_2O_3
Matrix	1	0,92	0,48	0,091	-0,064	0,22	0,18	0,056	n/a	0,013
	2	0,98	-0,67	-0,19	-0,0078	0,22	0,18	0,088	n/a	0,0042
	3	1,00	-0,10	-0,58	-0,019	0,49	0,13	0,11	n/a	-0,090
EA	1	0,99	-0,0026	n/a	n/a	-0,027	n/a	n/a	0,0053	0,0043
	2	0,99	-0,24	n/a	n/a	0,54	n/a	n/a	-0,076	-0,011
	3	1	-0,12	n/a	n/a	-0,84	n/a	n/a	-0,013	0,023
Matrix & EA	1	0,93	-0,021	-0,023	0,046	-0,037	-0,0010	-0,0036	-0,020	-0,069
	2	0,98	-0,018	-0,13	0,027	0,11	0,00066	0,0092	-0,069	-0,042
	3	0,99	-0,082	-0,23	-0,20	-0,24	-0,034	0,073	0,31	0,37
	8	1	0,60	-0,13	-0,57	0,36	0,29	0,19	0,68	0,72

To verify either an anthropogenic and non-anthropogenic origin for the enriched areas (EA), the data-set was standarized and statistically evaluated using discriminant analysis (DA). The data were categorized into three sets: (1) non-ablated silica matrix, (2) ablated silica matrix and (3) non-ablated enriched area (refer with Tab. 3). Since it is probable that contamination during curation was responsible for carbon (C) weight fractions presence (attaching the tools with a measuring table using a carbon tape or the presence of an egzogenic, organic surface impurities), they were not included in the DA model. The weights fractions below a detection limit (DL) were replaced by a value equal to its half (½ DL=0,05 wt%).

The results showed a very clear (Λ_W= 0,0000000) intergroup diversity within the silica matrices (Fig. 6a). With an exception of the K_3, K_4 and K_6, no significant differences were found between the non-ablated matrices and those ablated. A discrimination of the matrices of these three artifacts was made by the first and second canonical roots which are both correlated with MgO and P_2O_5 (refer with Tab. 3).

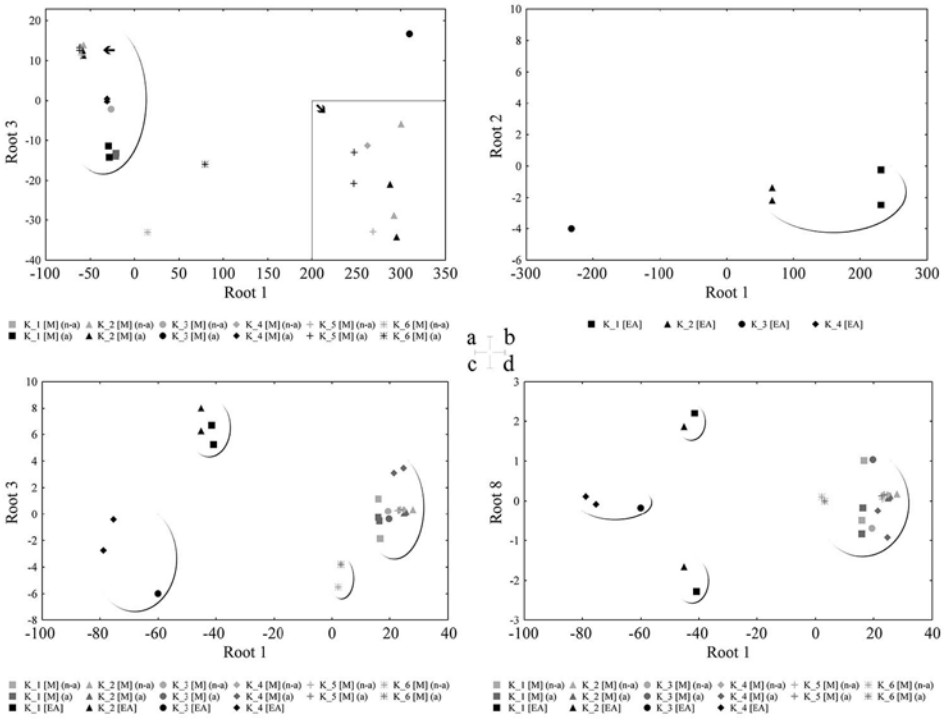

Fig. 6. The DA projections of the analythical areas: (a) the non-ablated and the ablated silica matrices on a root-plane 1–3; (b) the K_1–4 EA on a root-plane 1–2; (c) the silica matrices and the EA on a root-plane 1–3; (d) the silica matrices and the EA on a root-plane 1–8. Graphic design: Ł. Kowalski.

Given that the presence of the enriched areas (EA) on the K_5 and K_6 surfaces was not recognized by SEM-EDS (refer with Tab. 2) they were not included in the final DA model dedicated exclusively to EA. We found that the EA intergroup discrimination was of a high diversity (Λ_W= 0,0000001). K_1 and K_2 were agglomerating together and were separated from the K_3 and K_4 (Fig. 6b). Such a discrimination was made by positive (K_1 and K_2) and negative (K_3 and K_4) values of the first canonical root which is positively correlated with P_2O_5 and MnO (Tab. 3).

For all analytical areas, the DA results showed a very clear intergroup diversity (Λ_W=0,0000000). The K_1 and K_2 were agglomerating together nearby the K_3 and K_4. The enriched areas (EA) and the silica matrices areas (M) were separated from each other by negative (EA) and positive (M) values of the first canonical root (Fig. 6c). It is negatively correlated with Fe_2O_3 and positively with SiO_2 (refer with Tab. 3). The major contribution in the EA intergroup discrimination was made by the third canonacal root which is positively correlated with Fe_2O_3 and negatively with P_2O_5 and Al_2O_3 (refer with Tab. 3). Having been positively correlated with Fe_2O_3, MnO and MgO (refer with Tab. 3) the eighth canonical root generated an intragroup discriminant space for the K_1 and K_2 (Fig. 6d).

Normalized oxide weight fractions (=quantitative variables) were standarized and evaluated with a cluster analysis (CA) using Ward's linkage and Czebyshev's distance (Fig. 7a). The resulting distance matrix was used to perform multidimensional scaling (MDS). By means of the MDS a scatter plot bringing all the quantitative variables into relationship was generated (Fig. 7 b).

The results were used to plot the enriched areas (EA) on the ternary diagrams including the following scatter triads: CaO, P_2O_5, MnO and CaO, MgO, K_2O both with respect to Fe_2O_3 content. The oxide weight fractions were ranged in the range of <0, 1>. Due to P_2O_5 and MnO the first ternary scatter plot kept the K_1 and K_2 separate from the K_3 and K_4 (Fig. 7c). It was also found that contributions to the discrimination model was made by CaO and K_2O (Fig. 7d).

DISCUSSION

No significant qualitative differences were found between the chemical profiles of the non-ablated matrices and those ablated. Such an assumption however is not applicable to K_3 and K_4 since it was established that the differences recognized here are of a qualitative nature (presence of MgO and K_2O in the ablated matrices respectively). A tendency of decreasing carbon (C) amounts in the ablated matrices of the K_1, K_2, K_5 and K_6 and increasing in the K_3 and K_4 is quite noticeable. In K_3 and K_4, the increasing carbon could be due to its endogenic nature (=an accessory component) and it may be found in even-aged (syngenetic) growth of raw flint surrounded by organic silica (Bolewski and Parachoniak 1982: 322; Ryka and Maliszewska 1982: 171). The results are in accordance

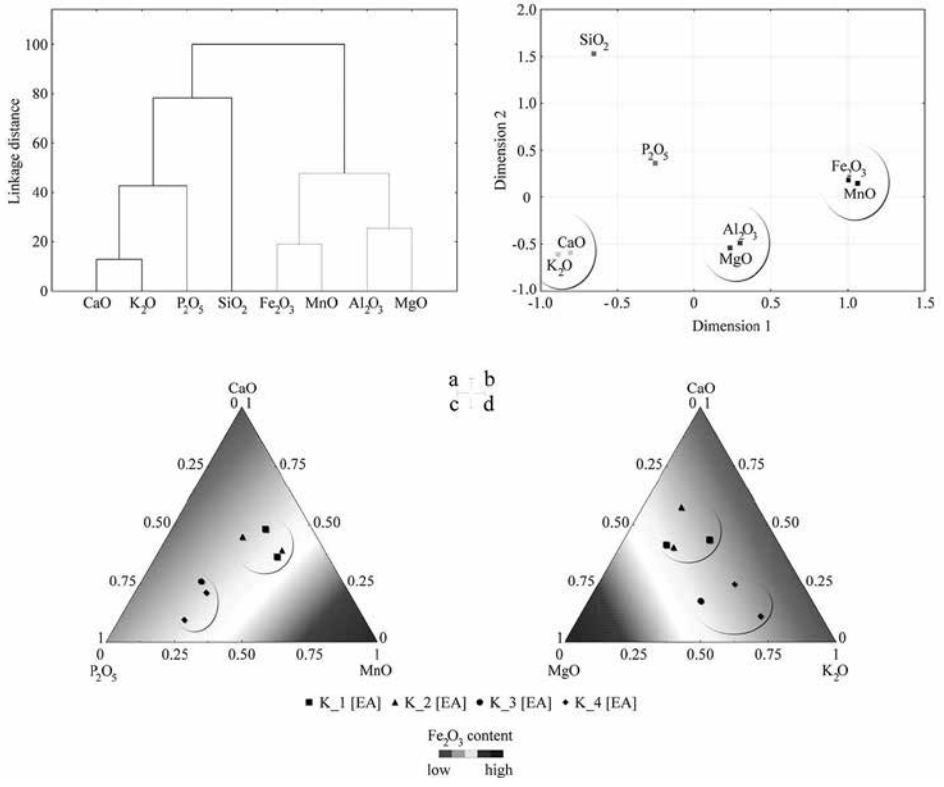

Fig. 7. (a) A dendrogram clustering the quantitative variables with Ward's linkage and Czebyshev's distance; (b) a scatter-plot for the quantitative variables on a 1–2 dimension-plane according to the MDS; (c) a ternary scatter plot for the EA on a CaO-P2O5-MnO plane and (d) CaO-MgO-K2O plane both with Fe2O3 content given as a linear function of corresponding oxides weight fractions. Graphic design: Ł. Kowalski.

with a tendency of K_2O and CaO to increase in these areas (= inclusions; Fig. 7a, b and d). For the rest of the samples, an increased carbon amount is probably of the egzogenic nature and thus may be seen as brought by anthropogenic (prehistoric or modern usage) or non-anthropogenic (epigenetic or post-depositional process) factors (refer with Anderson-Gerfaud 1984 and see also van Gijn 1989).

Presence of the enriched areas (EA) has not been recognized for the K_5 and K_6 samples during the SEM-EDS investigations. It is also not possible in the current study to indicate significant qualitative differences between the chemical profiles of the non-ablated matrices and those ablated. Nevertheless, the presence of such areas has been confirmed by the macroscopic observations (Fig. 5i–l). On the basis of the findings it is higly likely that these areas should be treated as natural inclusions in the silica matrices. The observation is analogous to the one from the K_3 and K_4. Since no significant dif-

ferences were found between the chemical profiles of the K_4 non-ablated or the ablated EA, it is most probable that this area is not of a residual but inclusion nature. Having been not arranged linearly, neither increase on the edges nor in the microdepressions the distribution of Fe on the K_4 surface (Fig. 5i and l) supports such an assumption. By means of the similarity analysis it is likely to be a chemical profile matching between the K_3 and K_4 EA allowing us to treat them both as inclusions.

It is noticeable that Al_2O_3 decreases in the ablated matrices of the K_5 and K_6. For the rest samples, Al_2O_3 is tend to increase, both in ablated matrices and the enriched areas (EA). The presence of phosphorus (P) in the K_3 and K_4 enriched areas may therefore be a consequence of P-Fe-Al mineral inclusions, such as vivianite or glauconite (Ryka and Maliszewska 1982: 171–172; Brzeziński *et al.*, 1983: 278; Sapek 2014: 86; Stolarczyk and Drewnik 2014: 58).

With a major contribution made by MnO and P_2O_5 a significant discrimination of the K_1 and K_2 enriched areas (EA) has been established (Fig. 6b–d and Fig. 7c and d). Having increased Al_2O_3 together with a presence of MgO the K_1 and K_2 EA are even more likely to be of a none genetic connection with the silica matrices. Such a conclusion is also supported by the MDS results indicating a Fe_2O_3 and MnO co-variance (Fig. 7a and b). Given that iron (Fe) has a lower redox potential than manganese (Mn) and phosphorus (P), which means that P and Mn are more stable than Fe under the same physicochemical conditions (Sadowski 1997: 760; Evans and Donahue 2005: 1739) and also that phosphorus tends to accumulate in the high-Fe genetic levels (Sapek 2014: 87), it must be recognized that residues present on the K_1 and K_2 had already been phosphorus-free originally and should be therefore treated as anthropogenic in nature. The results generated by use-wear analysis are crucial indicating that the residues are present on areas just adjacent to the use-worn zone (smoothest) and tend to be located in microdepressions of the microstructures (Fig. 4 and Fig. 5). Such a localization indicates the residues are not epipgenic nor are a result of post-depositional soil deposits (refer with Anderson-Gerfaud 1984).

Due to the chemical profile of the residues preserved on the K_1 and K_2 it is highly likely that they represent an ochre-type material (=red ore, i.e. hematite and limonite gravel). As we know, ochre is a limonite rock containing some impurities including (1) clay minerals (SiO_2, Al_2O_3 and MgO presence in the EA), (2) fine-grained quartz (SiO_2 presence in the EA) and (3) organic remains (enhancement of C in the EA). Importantly, goethite is the main component of the limonite and theoretically contains about 63 wt% of Fe (more than 40 wt% amount of Fe_2O_3 in the EA) with up to 5 wt% of Mn (MnO presence in the EA) and mechanical SiO_2 (SiO_2 presence in the EA; Bolewski and Parachoniak 1982: 331–333; Bolewski and Manecki 1993: 180–183 and see also Hensel 2011). The strong probability that the material identified is ochre accords with the results of use-wear analysis indicating that the use-wear traces were left by the prehistoric people who worked the abrasive ochre-type material (Fig. 4).

FINAL REMARKS

An integrated, multidisciplinary approach used in this study allowed direct identification of the use-wear traces and residues accumulated on a sample of functional tools collected from the Sąspów and Wierzbica 'Zele' flint mines sites. Although the SEM-EDS is a semi-quantitative analytical method, by applicating both the use-wear analysis and similarity analysis we were able to fingerprint the anthropogenic nature of the residues preserved on two of the functional tools analyzed.

REFERENCES

Anderson-Gerfaud, P. 1984. A few comments concerning residue analysis of stone plant-processing tools. In L.R. Owen and G. Unrath (eds), *Technical aspects of microwear studies of stone tools, Part I*, 69–87. Early Man News 9/10/11. Tübingen.

Bolewski, A. and Manecki, A. 1993. *Mineralogia szczegółowa*. Warszawa.

Bolewski, A. and Parachoniak, W. 1982. *Petrografia*. Warszawa.

Brzeziński,W., Dulinicz, M. and Kobyliński, Z. 1983. Zawartość fosforu w glebie jako wskaźnik dawnej działalności ludzkiej. *Kwartalnik Historii Kultury Materialnej* 31(3): 277–297.

Dzieduszycka-Machnikowa, A. and Lech, J. 1976. *Neolityczne zespoły pracowniane z kopalni krzemienia w Sąspowie*. Wrocław. Polskie Badania Archeologiczne 19.

Evans, A.A. and Donahue, R.E. 2005. The elemental chemistry of lithic microwear: an experiment. *Journal of Archaeological Science* 32: 1733–1740.

van Gijn, A.L. 1989. The wear and tear of flint. Principles of functional analysis applied to Dutch Neolithic assemblages. *Analecta Praehistorica Leidensia* 22: 1–181.

Hensel, Z. 2011. Physical and chemical examination of hematite gravel from Rydno Quarry and the Final Paleolithic campsites of Całowanie. In R. Schild, H. Królik, A.J. Tomaszewski and E. Ciepielewska (eds), *Rydno. A Stone Age red ochre quarry and socioeconomic center. A century of research*, 405–407. Warszawa.

Lech, H. and J. 1995. PL 3 Wierzbica 'Zele', Radom Province. *Archaeologia Polona* 33: 463–480.

Małecka-Kukawka, J. 2011. Problem of the flint tools from the Sąspów mine site in the light of use-wear analysis. In M. Capote, S. Consuegra, P. Díaz-del-Río and X. Terradas (eds), *Proceedings of the 2nd International Conference of the UISPP Commission on Flint Mining in Pre- and Protohistoric Times (Madrid, 14-17 October 2009)*, 139–147. Oxford. British Archaeological Repots. International Series 2260.

Małecka-Kukawka, J. 2012. Traseologia – badanie mikrośladów. In S. Tabaczyński, A. Marciniak, D. Cyngot and A. Zalewska (eds), *Przeszłość społeczna. Próba konceptualizacji*, 464–471. Poznań.

Ryka, W. and Maliszewska, A. 1982. *Słownik petrograficzny*. Warszawa.

Sadowski, Z. 1997. Biogeochemistry of iron and manganese. *Wiadomości Chemiczne* 51 (11–12): 758–770.

Sapek, B. 2014. Soil phosphorus accumulation and release – sources, processes, causes. *Water-Environment-Rural Areas* 14 (1): 77–100.

Stolarczyk, M. and Drewnik, M. 2014. Diversity of different fractions of phosphorus in grassland soils of agricultural lands in the vicinity of a fertilizer stockpile in Tarnawa Wyżna (Western Bieszczady Mts). *Prace Geograficzne* 135: 57–71.